

Restart uncertainty relation for monitored quantum dynamics

Ruoyu Yin,^{1,*} Qingyuan Wang,^{1,†} Sabine Tornow,^{2,‡} and Eli Barkai^{1,§}

¹*Department of Physics, Institute of Nanotechnology and Advanced Materials, Bar-Ilan University, Ramat-Gan 52900, Israel*

²*Research Institute CODE, University of the Bundeswehr Munich, 81739 Munich, Germany*

We introduce a novel time-energy uncertainty relationship within the context of restarts in monitored quantum dynamics. Initially, we investigate the concept of “first hitting time” in quantum systems using an IBM quantum computer and a three-site ring graph as our starting point. Previous studies have established that the mean recurrence time, which represents the time taken to return to the initial state, is quantized as an integer multiple of the sampling time, displaying pointwise discontinuous transitions at resonances. Our findings demonstrate that, the natural utilization of the restart mechanism in laboratory experiments, driven by finite data collection time spans, leads to a broadening effect on the transitions of the mean recurrence time. Our newly proposed uncertainty relation captures the underlying essence of these phenomena, by connecting the broadening of the mean hitting time near resonances, to the intrinsic energies of the quantum system and to the fluctuations of recurrence time. This work not only contributes to our understanding of fundamental aspects related to quantum measurements and dynamics, but also offers practical insights for the design of efficient quantum algorithms with mid-circuit measurements.

The concept of restarting a process is a ubiquitous phenomenon across various disciplines [1–3]. When faced with a setback in reaching a desired goal, the instinct to restart the process often arises, driven by the hope of achieving better success in subsequent attempts. This notion of restarting, or “resetting”, gives rise to a compelling paradigm in the realm of classical stochastic processes [2–18]. Diffusion processes with resets are the best-studied example [2]. In this scenario, a particle undergoes random diffusion but, at periodic or random intervals, is brought back to its initial position. Additionally, within this framework, a specific target awaits the particle’s arrival, prompting us to inquire about the time it takes for the particle to reach this target for the first time. This random time, both with and without the restart mechanism, is commonly known as the “first passage time” and has garnered widespread attention [19]. In particular, the notion of restarts plays a pivotal role in expediting search processes, making these ideas highly relevant and applicable across diverse fields, including biology [20], computer science [21, 22], animal foraging [23–25], the study of chemical reactions [26, 27], and quantum dynamics [28–45], among others.

The concept of restarting processes is of particular importance in the context of repeated mid-circuit measurements performed on quantum computers and more generally in the context of monitored quantum walks [46]. In quantum dynamics, the notion of “first hitting time” without restart reveals intriguing and novel features, often intimately connected with topological considerations, resonances, and the concept of dark states [46–68]. Typically, these processes are represented using graphs, which can describe the states of various quantum systems, such as single particles or qubit systems. Within this graph, a crucial element is the presence of a target state, often symbolizing the measurement device.

To detect the system at the target state, it might

be tempting to perform measurements at infinitesimally short intervals. However, this approach encounters the Zeno effect [69], where frequent strong measurements effectively freeze the system’s dynamics, rendering it undetectable. As a solution, a sequence of measurements is performed at regular intervals of τ units of time, allowing the system to evolve unitarily between measurements [46–50]. Yet, when implementing this fundamental search process on a quantum computer or any practical device, practical challenges emerge. Over time, due to measurement imperfections or interactions with the environment, quantum effects tend to diminish due to noise and decoherence. In such cases, a common strategy is to restart the process. This issue of finite-time resolution is not exclusive to the quantum realm and is encountered in classical systems as well. What distinguishes the quantum realm is the potential for sharp and discontinuous resonances in mean hitting times, related to quantum revivals [70] and topological effects (see below). Remarkably, as shown below, even when the restart time is significantly longer than the mean first hitting time, the act of restarting can have a profound impact. Our objective is to investigate these phenomena by leveraging a new uncertainty relation, which is vastly different from previous ones [71–76].

To illustrate the key aspects of our study, we commence with an experimental demonstration conducted on an IBM quantum computer. In this experiment, we consider a straightforward three-site ring graph with quantum states represented as $|0\rangle$, $|1\rangle$, and $|2\rangle$, as shown in Fig. 1. The system is described by a tight-binding Hamiltonian that accounts for hopping between these states. Our starting point is state $|0\rangle$, which also serves as the target state for this investigation. We aim to observe the recurrence of the system to its initial state through periodic measurements conducted every τ unit of time. The measurement outcomes yield a sequence of “no” re-

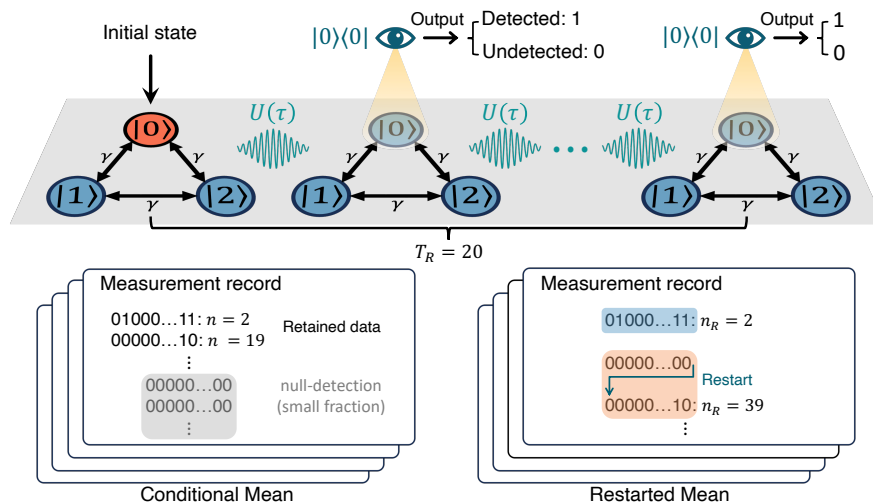


FIG. 1. **The measurement protocol for monitored quantum walks and its output.** The model of a tight-binding three-site ring is initialized at the spatial state $|0\rangle$ (colored orange). A projective measurement at the initial state, schematically presented by the eye symbol, is performed following the unitary evolution of time τ . The output of the measurement is either “yes” (1) or “no” (0), rendering the wavefunction of the quantum walker either localized at $|0\rangle$ or its amplitude erased at the state $|0\rangle$. We continue the free evolution immediately after the measurement for another duration τ , and then measure again, resulting in another binary outcome: 0 or 1. Using an IBM quantum computer the process of interrupting evolution by stroboscopic measurements was implemented for 20 steps, as a single realization, thus leading to an output string or measurement record of 20 bits. Our goal is to find the number of steps when the first 1 (“yes”) emerges, which is the quantum first hitting time in units of τ . Repeating a large number of realizations gives the statistics of hitting times. Two common statistical measures of estimating the mean hitting time are used. In the first we disregard the (rare) sequences with all 0 measurements, and this yields the mean conditioned on detection. In the second, called restarted hitting time, we continue until the first detection, as illustrated in the figure, leading to the sampling of the mean restarted hitting time. In this example the restart time is $T_R = 20$ in units of τ .

sponses (indicating null detection) followed by a “yes” response when the target state is eventually detected. The first occurrence of “yes” in this sequence defines the first hitting time [46–50], as demonstrated in Fig. 1. For instance, an experimental outcome might yield the sequence $\{no, no, yes\}$, which corresponds to a first detection time of 3τ . Through repeated experiments conducted on the quantum computer, we determine the mean number of measurements required for detection, denoted as $\langle n \rangle$. This quantity, extracted from the quantum computer, provides us with valuable insight into the average time it takes to detect the target state.

Theoretical investigations, spanning a wide range of graph types, have extensively explored the aforementioned problem [46–60, 64–66]. We first present the basic theory ignoring restart, showing that such a theory does not align with the experiments. Notably, Grünbaum and colleagues [46] made a remarkable discovery: the theoretical mean recurrence time exhibits quantization. In practical terms, this implies that the value of $\langle n \rangle$ is constrained to integer values. Mathematically, this integer is encapsulated by a winding number w associated with a generating function and hence the phenomenon is topo-

logical. The integer is defined and denoted as

$$\langle n \rangle = \sum_{n=1}^{\infty} n F_n = w. \quad (1)$$

Here F_n is the probability of first detection in the n -th measurement, which is normalized, i.e. $\sum_{n=1}^{\infty} F_n = 1$. It is obtained using the unitary $U(\tau) = \exp(-iH\tau)$ (\hbar is set as 1, and H is the Hamiltonian) describing the evolution between measurements and the projection $|0\rangle\langle 0|$ describing the measurements using collapse theory, so all along this work $|0\rangle$ is the target state. Specifically [46, 48, 50],

$$F_n = |\langle 0|U(\tau)\mathcal{S}^{n-1}|0\rangle|^2, \quad (2)$$

where the survival operator $\mathcal{S} = (\mathbb{1} - |0\rangle\langle 0|)U(\tau)$ ($\mathbb{1}$ is the identity matrix), demonstrating the unitary evolution in the time interval τ followed by the complementary projection described by $\mathbb{1} - |0\rangle\langle 0|$ (indicating null detection). In general, the winding number w is computed as follows [46, 53]: Given the time-independent Hamiltonian and assuming a finite graph, we search for the energy levels and corresponding states of the system, denoted as $H|E_k\rangle = E_k|E_k\rangle$. The value of $\langle n \rangle = w$ represents the count of distinct phase factors, such as $e^{-iE_k\tau}$, associated with stationary states that exhibit nonzero overlap with the target state.

In our experimental example on the three-site ring (see Methods Model), we encounter energy level degeneracy, resulting in $\langle n \rangle = 2$ for nearly any choice of τ . However, a pivotal observation emerges when the phase factors merge, causing $\langle n \rangle$ to become equal to 1. The merging of phase factors occurs for specific values of τ which are straightforward to identify. Consequently, the relationship between $\langle n \rangle$ and τ is predominantly characterized by the value 2, except for isolated pointwise discontinuities, where it abruptly becomes 1. These peculiar values of τ correspond to instances of wave packet revivals, wherein certain times lead to the complete revival of the wave packet to its initial state. During such moments, the first measurement invariably yields a “yes” outcome. What makes this phenomenon particularly extraordinary is the discontinuous nature of $\langle n \rangle$ and its intriguing insensitivity to values of τ beyond the revival times themselves.

The theoretical findings described above are valid in principle for infinitely long time measurements, and they have been graphically represented in Fig. 2, alongside the corresponding experimental results from an IBM Eagle processor (IBM Sherbrooke). Notably, the delta-like narrow transitions predicted by the theory are observed to exhibit widening in the real-world experimental data. Nonetheless, a clear alignment between theory and experiment persists, except in the immediate vicinity of these transitions. Importantly, the above-mentioned resonances and broadening effect is a generic phenomenon of first hitting time statistics, and is not limited to the example under study.

The inception of this research stemmed from the natural inquiry: Is this widening phenomenon a generic occurrence? Is it primarily attributed to inherent noise inherent to the system, such as imperfect timing in measurements or the unitary itself or is it potentially linked to the fundamental principles of quantum measurement theory? Specifically, can the basic postulates of quantum measurement theory provide a quantitative description of these transitions? When we refer to a “transition”, or a “topological transition” or “resonance”, we mean the shift of $\langle n \rangle = w$ (as illustrated by $w = 2$ in Fig. 2) to $\langle n \rangle = w - 1$ and back, as we systematically vary the parameter τ . In this context, τ serves as our control parameter, although it is worth noting that other parameters of the system Hamiltonian could be employed for a similar investigation. We claim below that the widening effects seen in Fig. 2, are generic and are due to the restart paradigm. Secondly, we find that the widening effects are determined by the fluctuations in the system, or to put it differently, the width of the transition teaches us about the fluctuations of the hitting time. Further, these uncertainties in hitting times are shown to be related to the energies of the system, thus extending the time-energy uncertainty relation to a case where the time is actually fluctuating.

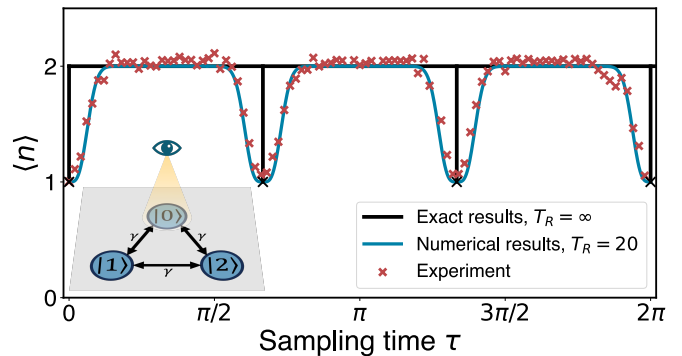


FIG. 2. Mean Hitting Time for the Three-Site Ring Model. The numerically/experimentally obtained mean quantum first return time of the three-site ring model. The exact results for $T_R = \infty$ (black line), as stated under equation (1), present discontinuous jumps or dips of $\langle n \rangle = w$, from $w = 2$ to $w = 1$, at $\tau = 2\pi k/3$ ($k = 0, 1, 2, \dots$). In the experimental data (red crosses, $T_R = 20$), these transitions are widened. The numerical results for $T_R = 20$ (blue line) perfectly match the experimental results. In the paper, we address the broadening effect showing how it is related to an uncertainty relation. Inset is the scheme of the tight-binding model for a ring with three sites, and γ denotes the strength of the hopping matrix element. We measure periodically the target state $|0\rangle$ (indicated with an eye). See details of the IBM remote experiments in Methods, and Supplementary Information (SI).

Results

Using mid-circuit measurements, the experimental output typically commences with a sequence of null measurements, characterized by the string $\{no, no, \dots\}$. It is important to note that this string is always finite, and its length is denoted as T_R (with the subscript “R” signifying “restart”). In some instances, we encounter a “yes” in the sequence, signifying the successful detection of interest, and thus providing the random hitting time. However, there are cases where we find a sequence composed entirely of “no’s”, implying that no detection has occurred until the time $T_R\tau$, see Fig. 1 with $T_R = 20$. To analyze the statistical features of the experiments, we use basics of restart theory. When we average the results, we focus on two essential statistical measures. The first is the mean, conditioned on detection within the first T_R attempts, denoted as $\langle n \rangle_{\text{Con}}$, is given by:

$$\langle n \rangle_{\text{Con}} = \frac{\sum_{n=1}^{T_R} n F_n}{\sum_{n=1}^{T_R} F_n}. \quad (3)$$

In the estimation of this mean, we exclude all sequences that contain T_R null measurements. The second statistical measure is the restarted mean, which counts all sequences, including those without any “yes”, denoted as $\langle n_R \rangle$. Namely, n_R gives the total number of attempts until the first “yes”, regardless of how many restarts have happened. See the schematics in Fig. 1. Its mean is

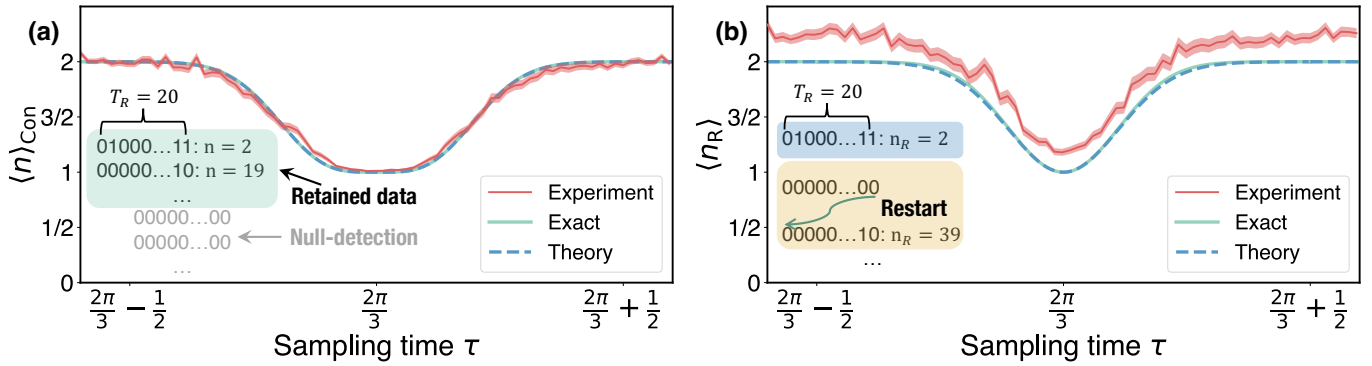


FIG. 3. **Impact of Restart on Hitting Time Transitions.** (a) The transition from $\langle n \rangle_{\text{Con}} = 2$ to $\langle n \rangle_{\text{Con}} = 1$ and back is widened due to restarts. In particular, here we restart after $T_R = 20$ measurements, as highlighted in the insets. We compare the exact results (gray solid line) found using equations (2,3) with the theory (blue dashed line) obtained using equation (6) and IBM quantum computer experiments (red line). The results clearly demonstrate that basic postulates of measurement theory and the uncertainty relation using the variance of the hitting time perfectly align with the experiment. In turn, noise and imperfect measurements are not factors in the observed behaviour. (b) The mean hitting time under restart, $\langle n_R \rangle$, as a function of τ . We compare the exact results (gray solid line), the theory (blue dashed line, computed with equation (7)) and experiment results on the IBM quantum computer (red line) for $T_R = 20$. We observe the vertical shift between the experimental and exact results, which is due to noise in quantum computers, and more specifically, due to a small 1% shift in the detection probability which is discussed in the text. The model here is a tight-binding three-site ring, the same as in Fig. 2. In both figures, the exact results are obtained using equation (2), from which we find F_n , and then using equation (3) for (a) or equation (4) for (b). The shaded red region represents the confidence interval 99.7%, signifying an interval spanning three standard deviations above and below the mean in a standard normal distribution.

quantified as [37, 77]:

$$\langle n_R \rangle = \langle n \rangle_{\text{Con}} + T_R \frac{1 - \sum_{n=1}^{T_R} F_n}{\sum_{n=1}^{T_R} F_n}, \quad (4)$$

Here, the first term on the right-hand side corresponds to paths where detection occurred within T_R attempts, while the second term encompasses paths where detection happened after T_R attempts. Therefore, the mean restart time, $\langle n_R \rangle \tau$, provides an estimate of the average time until the first detection, considering an ensemble that does not exclude any specific path. In theory, as T_R tends toward infinity, we obtain the idealized limit as expressed in equation (1) from equations (3) and (4), though precisely in the vicinity of resonances, this limit must be considered with care.

We introduce the variance of detection times, measured in units of τ , as:

$$\sigma_n^2 = \langle n^2 \rangle - \langle n \rangle^2 = \sum_{n=1}^{\infty} n^2 F_n - w^2. \quad (5)$$

This variance, denoted as σ_n^2 , quantifies the uncertainty associated with the first hitting time. Importantly, this uncertainty tends to be substantial in the proximity of the topological transition under investigation, and notably, these fluctuations become more pronounced as we approach the transition [53]. Our main results are relationships between this uncertainty and the restarted

process using the following expressions:

$$\langle n \rangle_{\text{Con}} = w - \left(\frac{2T_R}{\sigma_n^2} + 1 \right) \exp \left(-\frac{2T_R}{\sigma_n^2} \right), \quad (6)$$

$$\langle n_R \rangle = w - \exp \left(-\frac{2T_R}{\sigma_n^2} \right). \quad (7)$$

These equations hold in the limit of large T_R and large σ_n^2 while keeping the ratio T_R/σ_n^2 constant. These relationships are general in nature, describing transitions from w to $w - 1$, a phenomenon found in a broad class of Hamiltonians when a pair of phase factors merge. When $T_R/\sigma_n^2 \rightarrow \infty$, signifying a state far from resonance, we observe that $\langle n \rangle_{\text{Con}} = \langle n_R \rangle = w$. Conversely, when $T_R/\sigma_n^2 \rightarrow 0$, indicating resonance, we find that $\langle n \rangle_{\text{Con}} = \langle n_R \rangle = w - 1$. Thus, equations (6,7) describe the broadening of the transitions that diminishes as we increase the resetting time. These findings are significant as many aspects of the process, such as the complete spectrum of \mathcal{S} or U , are unimportant and do not impact the overall outcome. We will soon show that this is related to a new type of time-energy relation.

Experimental validation

In the analysis of the experimental data depicted in Fig. 3(a), we relied on the use of the conditional mean, as described earlier. Additionally, we provided a theoretical representation based on equation (6), which ex-

hibits a remarkable alignment with the experimental results without requiring any fitting procedures. This indicates that the uncertainty relation, solely based on measurement postulates and not noise in the IBM quantum computer, is responsible for the broadening. For these experiments, we set $T_R = 20$. Interestingly, in Fig. 3(b), for the restarted mean, we also observe an alignment of the theory with experiment, though now we see a small constant shift between predictions and the data. We now explain this effect.

Consider τ in Fig. 3(b) far from resonance, for instance, at $\tau = 2\pi/3$, the theoretical detection probability within time $T_R = 20$, $P_{\text{det}} = \sum_{n=1}^{T_R} F_n$, is approximately equal to 1. However, in our experimental observations, we find that P_{det} is approximately 0.99, indicating a small but notable deviation between theory and experiment. This slight deviation has a noticeable impact on the expected value of n_R . Recall that $(1 - P_{\text{det}})T_R/P_{\text{det}}$, i.e. the second term in equation (4), is approximately 0, since $P_{\text{det}} \simeq 1$. However, when we use the experimental values just mentioned, we find that for $T_R = 20$, $T_R(1 - P_{\text{det}})/P_{\text{det}} = 0.2$. Remarkably, this observed value corresponds exactly to the shift we observe in $\langle n_R \rangle$, as presented in Fig. 3(b) (please refer to the Supplementary Note 1 in SI for an in-depth discussion on this issue). We conclude that the small shift is consistent with very small errors in the estimation of the detection probability P_{det} .

This situation highlights a crucial point: when T_R is large, even small errors on the order of 1% can result in a visible shift in the experimental outcome, $\langle n_R \rangle$, and this shift grows linearly with T_R . A similar effect is not found for the conditional mean. As mentioned, the latter neglects experimental realisations with no detections at all. The conditional mean consistently falls below the restarted mean, a trend particularly noteworthy in search contexts, where the primary objective is to expedite the process. Hence one should wonder which measure holds greater merit. We believe that both are valuable statistical measures, and there is no point in highlighting one over the other. Now, let us return to the theoretical analysis of the uncertainty relation. In a follow-up paper, we will study the noise and leakage of our circuit that led to the above-mentioned one percent deviation between the theoretical and experimentally found detection probability.

Uncertainty and Energy

Given that the merging energy phase factors, denoted $\exp(-iE_+\tau)$ and $\exp(-iE_-\tau)$, are responsible for the resonances observed, we aim to establish a connection between the restarted and conditional means and the underlying energies within the system. To accomplish this, we provide a sketch of the proof of the main results and extend them. In the limit of a large number of attempts (denoted as n), the probability of detection in the n -th

attempt exhibits exponential decay, as expressed by:

$$F_n \sim a(\zeta_{\text{max}}) |\zeta_{\text{max}}|^{2n}. \quad (8)$$

$|\zeta_{\text{max}}|$ is the largest eigenvalue of the survival operator \mathcal{S} satisfying $|\zeta_{\text{max}}| < 1$. $a(\zeta_{\text{max}})$ is a coefficient independent of n (which will soon be discussed). A critical aspect to consider is that when we precisely tune τ to the resonance, $|\zeta_{\text{max}}| \rightarrow 1$ (see below for graphic explanation) [46, 53, 54, 62]. As we soon explain at resonance $\lim_{|\zeta_{\text{max}}| \rightarrow 1} a(\zeta_{\text{max}}) = 0$. This occurrence effectively reduces the dimension of the Hilbert space, and this reduction can be demonstrated as the reason for the transition from w to $w - 1$ [46], which, in turn, translates to the resonance observed in the hitting time. To gain insight, let us consider a scenario in which two phase factors have exactly merged, specifically when $\exp(-iE_-\tau) = \exp(-iE_+\tau)$ for some pair of energy levels. In this case, the following state is called dark [54, 62]:

$$|D\rangle = N [\langle E_+ | 0 \rangle |E_-\rangle - \langle E_- | 0 \rangle |E_+\rangle]. \quad (9)$$

Here N is for normalization, and $\mathcal{S}|D\rangle = e^{-iE_+\tau}|D\rangle$, indicating that the eigenvalue of \mathcal{S} resides on the unit circle. Since this state is orthogonal to the target state $|0\rangle$ and also an eigenstate of the unitary, if we initially populate this state, it is never detected, so it is a dark state. Hence, when we adjust the parameter τ , which is the focus of our resonance and broadening study, we find that it is intricately linked to the creation of a dark state within the Hilbert space. Further, when the parameters are set close to resonance, $|\zeta_{\text{max}}|$ is close to unity, indicating a very slow relaxation of F_n , which in turn is responsible for the novel effects of the restarted process.

To continue consider the sum in the numerator of equation (3) using equations (1,8)

$$\begin{aligned} \sum_{n=1}^{T_R} nF_n &= w - \sum_{T_R}^{\infty} nF_n \\ &\sim w - a(\zeta_{\text{max}}) \frac{T_R (1 - |\zeta_{\text{max}}|^2) + 1}{(1 - |\zeta_{\text{max}}|^2)^2} |\zeta_{\text{max}}|^{2(1+T_R)}, \end{aligned} \quad (10)$$

where we summed an infinite series. As mentioned when phase factors match, the right-hand side of equation (10), according to the main theorem in the field [46] must be $w - 1$, when T_R is large. It then follows that, taking the limit $|\zeta_{\text{max}}| \rightarrow 1$ before $T_R \rightarrow \infty$ in equation (10), we find $a(\zeta_{\text{max}}) \sim (1 - |\zeta_{\text{max}}|^2)^2$, a result that can be reached with rigorous arguments. Applying a similar procedure to the denominator of equation (3) and to equation (4) leads to the following main result: let $\rho = T_R(1 - |\zeta_{\text{max}}|^2)$, when $|\zeta_{\text{max}}| \rightarrow 1$ and $T_R \rightarrow \infty$, we find

$$\langle n \rangle_{\text{Con}} = w - (\rho + 1)e^{-\rho} \text{ and } \langle n_R \rangle = \langle n \rangle_{\text{Con}} + \rho e^{-\rho}. \quad (11)$$

These formulas relate the resonances and the broadening to both the slowest decaying channel in the problem, i.e.

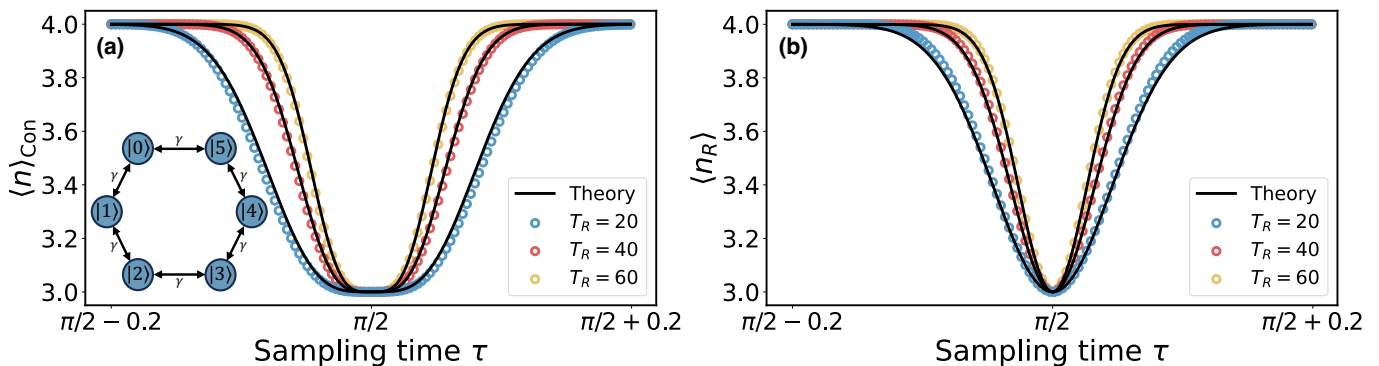


FIG. 4. **The Broadening of the Hitting Time Transitions in the Benzene-Type Ring Model.** (a) The conditional mean $\langle n \rangle_{\text{Con}}$ and (c) the restart mean $\langle n_R \rangle$ as a function of τ . The model here is the benzene-type ring (equation (16) with $L = 6$ and $\gamma = 1$), and we work in the vicinity of its critical sampling time $\tau = \pi/2$, with the transition $\langle n \rangle = 4$ to $\langle n \rangle = 3$. The black lines represent the theory from equations (6) and (7). The dots represent the numerical exact results obtained using equation (2). In the figures, from the bottom to the top line, the restart time T_R is 20, 40, and 60, respectively. Clearly, the transition is narrowed when T_R grows. Inset is the scheme of the benzene-type ring model, and the target state is $|0\rangle$.

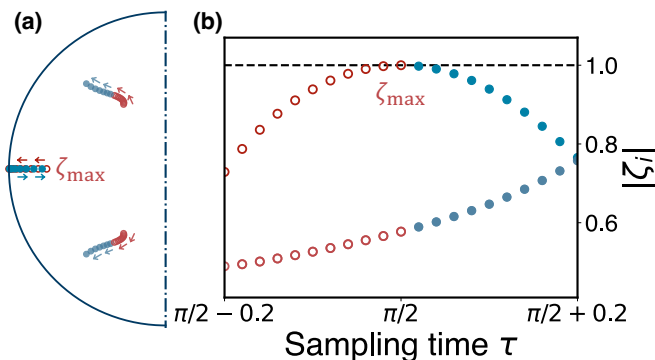


FIG. 5. **Eigenvalue Analysis in the Benzene-Type Ring Model.** The eigenvalues $\{\zeta_i\}$ of the survival operator \mathcal{S} for the six-site ring model, with the sampling time τ varied in the same range as in Fig. 4. Recall that $|\zeta_i|$ in general are less or equal unity. In (a) we present the eigenvalues as the sampling time τ is varied, and the semicircle is of radius 1. In (b) we plot the absolute values of $\{\zeta_i\}$. Due to the degeneracies of \mathcal{S} , we have three eigenvalues. As shown in (a), two eigenvalues (conjugate to each other) are far away from the unit circle and hence become irrelevant. One eigenvalue approaches the unit circle, and is solely responsible for the hitting time statistics and the uncertainty relation. We use arrows to illustrate entering or exiting the resonance at $\tau = \pi/2$. The red open circles present the eigenvalues when entering the resonance, and blue closed circles are used for the ones when exiting the resonance. The corresponding behaviors of the distance of the eigenvalues $\{\zeta_i\}$ to the origin are demonstrated in (b), where the two irrelevant eigenvalues share one set of data presented by the lower circles. Clearly, we see $|\zeta_{\text{max}}|$ goes to 1 and back when entering and exiting the resonance. As explained in the text, when $|\zeta_{\text{max}}| = 1$ we have a dark state in the system, see equation (9).

to the eigenvalue ζ_{max} , and the restart time T_R . They show how an analysis of the spectrum of the survival operator, in particular, the finding of its largest eigenvalue $|\zeta_{\text{max}}| < 1$, is crucial for the problem.

We now consider the fluctuations of the hitting time. Splitting the sum equation (5) into two, we have

$$\sigma_n^2 = \sum_{n=1}^{k_c} (n-w)^2 F_n + \sum_{k_c+1}^{\infty} (n-w)^2 F_n. \quad (12)$$

Choosing a large value of k_c such that we can use equation (8), summing an infinite series we find [53] $\sigma_n^2 \sim 2/(1 - |\zeta_{\text{max}}|^2)$. This quantifies the statement made before: the fluctuations are large close to the transition since $|\zeta_{\text{max}}| \simeq 1$. Using this relation between the uncertainty σ_n and the eigenvalue ζ_{max} we obtain equations (6,7). A rigorous proof, including the validity of equation (8), is provided in the Supplementary Note 2 in SI.

To complete the physical picture, namely, connect the resonance width with the energies of the system, we use the results in [53]. A perturbation theory, where the small parameter is the small arc on the unit disk, connecting the two nearly merging phases $\exp(-iE_-\tau)$ and $\exp(-iE_+\tau)$, was used to find ζ_{max} . The results in Ref. [53] gives $|\zeta_{\text{max}}|^2 \sim 1 - \lambda(\widetilde{\Delta E \tau})^2$ (parameters soon to be defined). Then with equation (11) we find

$$\langle n \rangle_{\text{Con}} = w - \left[1 + \lambda T_R (\widetilde{\Delta E \tau})^2 \right] \exp \left[-\lambda T_R (\widetilde{\Delta E \tau})^2 \right], \quad (13)$$

$$\langle n_R \rangle = w - \exp \left[-\lambda T_R (\widetilde{\Delta E \tau})^2 \right], \quad (14)$$

where $\lambda = p_+ p_- / (p_+ + p_-)^3$ with the overlaps $p_{\pm} = \sum_l^{g_{\pm}} |\langle 0 | E_{\pm, l} \rangle|^2$ (g_{\pm} is the degeneracy of the energy level E_{\pm}), and

$$\widetilde{\Delta E \tau} =: \tau |E_+ - E_-| \pmod{2\pi}. \quad (15)$$

Equations (13,14) clearly show the dependence of the mean hitting time on the system energies, and also practically, are employed to obtain the theoretical results in Fig. 3. At resonances, when $\widehat{\Delta E}\tau = 0$, both $\langle n \rangle_{\text{Con}}$ and $\langle n_R \rangle$ are equal to $w - 1$. Additionally, the resonance width decreases when we increase the restart time, assuming all other parameters remain constant.

We tested our theory using several model systems. For example, a benzene-type ring (equation (16) with $L = 6$), as presented in Fig. 4, where excellent agreement between the theory and numerically exact results is witnessed. We see, as predicted by equations (13,14), the width of the transition becomes smaller as the restart time T_R grows. To verify the uniqueness of ζ_{max} , in Fig. 5, we present the behaviors of the eigenvalues $\{\zeta_i\}$ for the model of benzene-type ring, when the sampling time τ is varied. One of the eigenvalues, namely ζ_{max} , approaches the unit circle when τ goes to $\pi/2$, while the other pair of conjugate eigenvalues are relatively far from the unit circle. As previously stated, when the largest eigenvalue $|\zeta_{\text{max}}|$ approaches the unit disk, the relevance of the other eigenvalues is negligible and the restart uncertainty relation presented in this work becomes relevant.

Discussion

In a broader perspective, the observed transitions exhibit similarities to line-shape resonances and broadening encountered across various fields of spectroscopy [78]. However, a distinguishing feature here is that the periodic driving force is not an external field acting upon a material system. Rather, they arise from the intrinsic nature of the measurements themselves and their periodicity. Notably, resonances are associated with the creation of dark states, in contrast to traditional resonances linked to quanta of energy carried by particles such as photons.

The broadening of these resonances is intricately linked to three crucial factors: the uncertainty σ_n , the slowest decaying mode in the problem, i.e. $|\zeta_{\text{max}}|$, and the energies of a pair of merging phase factors. This interconnection establishes fundamental relationships between quantum hitting time statistics and the system's underlying characteristics, with the restart time playing a pivotal role. It is noteworthy that analogous resonances may be present in related scenarios, particularly when we venture beyond the recurrence problem or engage in non-local measurements [61]. The expansion of our findings to encompass other observables and the exploration of cases where degeneracies are associated with the absolute value of the eigenvalue $|\zeta_{\text{max}}|$, resulting in non-pure exponential decay of F_n and transitions from $w \rightarrow w - 2$ or $w \rightarrow w - 3$, etc., rather than the studied $w \rightarrow w - 1$ case, represents an avenue for future research.

Additionally, we have devised a method for detecting resonances and quantifying their widths in the context of restarted hitting times on quantum computers. We anticipate this to be a valuable tool for investigating the inter-

play between mid-circuit measurements and unitary operations. The width of the resonance can serve as an indicator of whether the fundamental postulates of measurement theory are effectively functioning on a given device or if noise and decoherence are exerting control. In our experimental study, which was remotely conducted on an IBM quantum computer, we demonstrated that the former scenario holds true. However, we anticipate that, as we increase the size of the quantum system or adjust the restart time, distinct behaviors related to the coupling of these systems to the environment may emerge. Such insights will provide valuable information on the operating conditions of the new generation of algorithms with mid-circuit measurements, e.g. dynamic circuits [79].

The strategy of restarts used here is nearly mandatory for several reasons. In real quantum circuits, noise and leakage are present. Hence to study the quantumness of the problem, one is obliged to use finite-time experiments. More generally, unless one finds a way to perfectly correct noise and eliminate leakage in quantum computers with mid-circuit measurements, the restart strategy is nearly a must. The significance of the broadening effect becomes crucial close to discontinuous behaviours of the hitting time statistics, leading to a time-energy uncertainty relation deeply related to the variance of the first detection time. This insight, promisingly, holds the potential to contribute to a better understanding and design of efficient quantum algorithms, which rely on backtracking (restart) and monitored dynamics [80]. More importantly, we provided a restart hitting time uncertainty relation, and since hitting times are fluctuating, the uncertainty relation differs from the standard time-energy relation, where time is a parameter and not an observable.

Methods

Model

The example we considered in the main text is a ring model governed by the nearest-neighbor tight-binding Hamiltonian

$$H = -\gamma \sum_{j=0}^{L-1} (|x\rangle \langle x+1| + |x\rangle \langle x-1|), \quad (16)$$

where γ is the hopping amplitude, L is the size of the system, and $\{|x\rangle\}$ are the spatial states composing the ring system. As noted, the main results in the manuscript are generally valid and are not limited to this model. The periodical boundary condition indicates $|0\rangle = |L\rangle$, and $|0\rangle$ is the target state. The eigenvalues of the Hamiltonian (16) are

$$E_k = -2\gamma \cos \theta_k, \quad (17)$$

with $\theta_k = 2\pi k/L$ and $k = 0, 1, 2, \dots, L - 1$. The corresponding eigenstates are $|E_k\rangle = \sum_{x=0}^{L-1} e^{i\theta_k x} |x\rangle / \sqrt{L}$.

Hence the overlap is $|\langle x|E_k\rangle|^2 = 1/L$. In the main text, for simplicity, we set the hopping amplitude γ as 1.

The *three-site ring* was used in our remote IBM experiments. Using equation (17) with $L = 3$, there are 2 distinct energy levels, $\{-2, 1\}$, with $|\langle x|E_k\rangle|^2 = 1/3$ and the energy level $E_1 = E_2 = 1$ is doubly degenerate. Hence the overlaps are $p_- = 2/3$, and $p_+ = 1/3$. When $\tau = 2\pi j/3$ with $j = 0, 1, 2, \dots$, the mean $\langle n \rangle$ for $T_R \rightarrow \infty$ jumps from $w = 2$ to $w = 1$, where energy phases $\{e^{-i\tau}, e^{i2\tau}\}$ match. Using the above mentioned p_- and p_+ and energies, equations (13,14) give $\lambda = 2/9$, and $\widetilde{\Delta E\tau} = |3\tau - 2\pi j|$ close to each $\tau = 2\pi j/3$. In Fig. 3, $j = 1$ and the resonance condition $\tau = 2\pi/3$ is used. As mentioned, these jumps in the mean hitting time correspond to revivals of the wave packet on the origin.

The *benzene-type ring* was used in our examples plotted in Fig. 4. Here $L = 6$ and the distinct energies are $\{\pm 2, \pm 1\}$ where the energies ± 1 are two-fold degenerate. Hence the overlaps corresponding to distinct energies are $|\langle 0|E_0 = -2\rangle|^2 = |\langle 0|E_3 = 2\rangle|^2 = 1/6$, and $|\langle 0|E_1 = -1\rangle|^2 + |\langle 0|E_5 = -1\rangle|^2 = |\langle 0|E_2 = 1\rangle|^2 + |\langle 0|E_4 = 1\rangle|^2 = 1/3$. Using equation (1) we therefore expect that, except for a small subset of τ 's, $\langle n \rangle = 4$. When $\tau = (2j + 1)\pi/2$ with $j = 0, 1, 2, \dots$, $\langle n \rangle$ for $T_R \rightarrow \infty$ jumps from $w = 4$ to $w = 3$, where the energy phases $\{e^{i2\tau}, e^{-i2\tau}\}$ merge, hence E_+ and E_- used in the text are -2 and 2 , respectively. So the parameters in equations (13, 14) are, $\lambda = 3/4$, and $\widetilde{\Delta E\tau} = |4\tau - 2\pi(2j + 1)|$ close to each $\tau = (2j + 1)\pi/2$. In Fig. 4, $j = 0$ or $\tau = \pi/2$ is used.

Sketch of the rigorous proof for the uncertainty relation

To prove the uncertainty relation, the key is to validate equation (8). Briefly speaking, this can be done via the generating function method [50]. Applying the Z -transform to the expression inside the bracket of equation (2), i.e. $\phi_n = \langle 0|U(\tau)\mathcal{S}^{n-1}|0\rangle$, one can obtain the generating function, $\tilde{\phi}(z) = \sum_{n=1}^{\infty} z^n \phi_n$. Decomposed by the Hamiltonian's eigenstates, and being a polynomial, $\tilde{\phi}(z)$ can be factorized by its zeros and poles, using Blaschke factorization [46]. Due to the mathematical property of the latter, the poles are the reflection of the zeros, with respect to the unit circle. And also, the zeros are the complex conjugate of the eigenvalues, $\{\zeta_i\}$, of the survival operator \mathcal{S} (see Supplementary Note 2 in SI) [54]. Hence, the generating function $\tilde{\phi}(z)$ can be completely factorized by the zeros, or the eigenvalues $\{\zeta_i\}$. This allows us, in terms of $\{\zeta_i\}$, to use the residue theorem, to recover ϕ_n via the inversion formula $\phi_n = \frac{1}{2\pi i} \oint_{|z|=1} \tilde{\phi}(z) z^{-(n+1)} dz$. And then $F_n = |\phi_n|^2$ can be computed and simplified to equation (8). The detailed derivation is presented in the Supplementary Note 2 in SI.

Implementation on a quantum computer

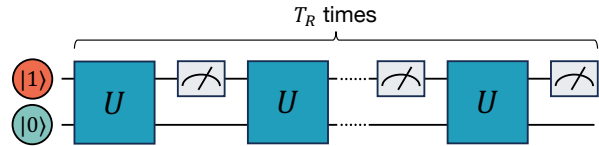


FIG. 6. **Quantum Circuit Representation for the Three-Site Ring Model.** Quantum circuit for two qubits representing the three localized states with alternating unitary U and measurements, with the initial state and target state $|0\rangle = |01\rangle$.

We design a three-site ring model, Fig. 2, using equation (16) with $L = 3$. To realise the three-site system on a quantum computer, we use two qubits, which can generate four states: $|00\rangle, |01\rangle, |10\rangle$ and $|11\rangle$. Hence, we employ the following mapping between the qubits and spatial states representation: $|01\rangle \rightarrow |0\rangle, |00\rangle \rightarrow |1\rangle$ and $|10\rangle \rightarrow |2\rangle$. We design our circuit in such a way that the additional state $|11\rangle$ is not connected to the others and will never be detected at least theoretically.

In our study we detect the state $|0\rangle \rightarrow |01\rangle$. This can be realised by measuring only the upper (right) qubit. Hence, when measuring the upper (right) qubit in state $|0\rangle$, the measurement does not give any information to distinguish the state $|1\rangle \rightarrow |10\rangle$ and $|2\rangle \rightarrow |00\rangle$. Importantly, measuring the upper (right) qubit in state $|1\rangle$ tells that the system is in $|0\rangle \rightarrow |01\rangle$ with certainty.

We determine the first detection time, n , by analysing mid-circuit measurement outputs from the quantum circuit, as shown in Fig. 6. We examine the expected value of n as a function of τ , considering the detection of the target state, namely the upper (right) qubit being detected in state $|1\rangle$, as the endpoint of measurement. As detailed earlier, measurements restart at finite T_R , yielding output strings like $\{0, 1, 0, 1, 1, \dots\}$, of length T_R , with “0” and “1” indicating the state of the upper (right) qubit, or actually failure and success in detection, respectively. The experiment ideally concludes after the first appearance of “1”, but due to technological constraints, we cannot terminate the quantum computation based on the measurement outputs, necessitating a finite and constant T_R .

The maximum duration for measurement repetitions in the IBM quantum computer is set at $T_R \simeq 20$. This restriction is influenced by software limitations specific to the quantum computer we used. This choice is also chosen to reduce noise and avert non-unitary actions and probability leakage. Such occurrences could render the system's Hamiltonian (H) effectively non-Hermitian (see our follow-up paper). In particular, when performing our experiments on IBM Sherbrooke, $T_R = 20$ was the maximum number of repeated measurements allowed by the software.

As shown in Fig. 1, to calculate the conditional mean $\langle n \rangle_{\text{Con}}$, we disregarded null-detection strings, which are strings of length twenty with only zeros $\{0, 0, \dots, 0\}$. Such strings are rare, since the P_{det} within 20 measurements is nearly 1 (at most 2 percent below 1, depending on τ), see details and figure for P_{det} in SI. For the restarted mean, we analyse the unconditional hitting time with restarts, noting the first detection time as n_R . For example, consider the sequence of $\{0, 0, \dots, 0\}$ of length 20, which, after a restart event, is followed by $\{0, 0, 1, \dots\}$. Here, the first time for detection under restart is $n_R = 23$. In total, we conducted 32,000 runs with $T_R = 20$ bits per run, requiring additional data processing to identify the first “1” in each string, thus obtaining the first hitting time n for each run. See the Supplementary Note 3 in SI for more details on the quantum circuit implementation, error suppression, and data processing.

* yinruoy@biu.ac.il

† qingwqy@gmail.com; These authors contributed equally to this work

‡ sabine.tornow@unibw.de

§ Eli.Barkai@biu.ac.il

- [1] M. R. Evans and S. N. Majumdar, *Journal of Physics A: Mathematical and Theoretical* **44**, 435001 (2011).
- [2] M. R. Evans and S. N. Majumdar, *Phys. Rev. Lett.* **106**, 160601 (2011).
- [3] A. Pal, V. Stojkoski, and T. Sandev, [arXiv:2310.12057](https://arxiv.org/abs/2310.12057) (2023).
- [4] A. Pal, *Phys. Rev. E* **91**, 012113 (2015).
- [5] A. Pal, A. Kundu, and M. R. Evans, *Journal of Physics A: Mathematical and Theoretical* **49**, 225001 (2016).
- [6] S. Eule and J. J. Metzger, *New Journal of Physics* **18**, 033006 (2016).
- [7] A. Pal and S. Reuveni, *Phys. Rev. Lett.* **118**, 030603 (2017).
- [8] S. Belan, *Phys. Rev. Lett.* **120**, 080601 (2018).
- [9] M. R. Evans and S. N. Majumdar, *Journal of Physics A: Mathematical and Theoretical* **51**, 475003 (2018).
- [10] A. Masó-Puigdellosas, D. Campos, and V. Méndez, *Frontiers in Physics* **7** (2019).
- [11] A. Pal, I. Eliazar, and S. Reuveni, *Phys. Rev. Lett.* **122**, 020602 (2019).
- [12] M. R. Evans, S. N. Majumdar, and G. Schehr, *Journal of Physics A: Mathematical and Theoretical* **53**, 193001 (2020).
- [13] O. Tal-Friedman, A. Pal, A. Sekhon, S. Reuveni, and Y. Roichman, *The Journal of Physical Chemistry Letters* **11**, 7350 (2020).
- [14] B. De Bruyne, J. Randon-Furling, and S. Redner, *Phys. Rev. Lett.* **125**, 050602 (2020).
- [15] D. Gupta, C. A. Plata, and A. Pal, *Phys. Rev. Lett.* **124**, 110608 (2020).
- [16] S. Gupta and A. M. Jayannavar, *Frontiers in Physics* **10** (2022).
- [17] W. Wang, A. G. Cherstvy, R. Metzler, and I. M. Sokolov, *Phys. Rev. Res.* **4**, 013161 (2022).
- [18] B. De Bruyne, S. N. Majumdar, and G. Schehr, *Phys. Rev. Lett.* **128**, 200603 (2022).
- [19] S. Redner, *A Guide to First-Passage Processes* (Cambridge University Press, 2001).
- [20] J. J. Hopfield, *Proceedings of the National Academy of Sciences* **71**, 4135 (1974).
- [21] M. Luby, A. Sinclair, and D. Zuckerman, in *[1993] The 2nd Israel Symposium on Theory and Computing Systems* (1993).
- [22] C. P. Gomes, B. Selman, and H. Kautz, in *Proceedings of the Fifteenth National/Tenth Conference on Artificial Intelligence/Innovative Applications of Artificial Intelligence*, AAAI '98/IAAI '98 (American Association for Artificial Intelligence, USA, 1998) p. 431–437.
- [23] D. Boyer and C. Solis-Salas, *Phys. Rev. Lett.* **112**, 240601 (2014).
- [24] G. Mercado-Vásquez and D. Boyer, *Journal of Physics A: Mathematical and Theoretical* **51**, 405601 (2018).
- [25] A. Pal, L. Kuśmierz, and S. Reuveni, *Phys. Rev. Res.* **2**, 043174 (2020).
- [26] G. Bel, B. Munsky, and I. Nemenman, *Physical Biology* **7**, 016003 (2009).
- [27] S. Reuveni, M. Urbakh, and J. Klafter, *Proceedings of the National Academy of Sciences* **111**, 4391 (2014).
- [28] B. Mukherjee, K. Sengupta, and S. N. Majumdar, *Phys. Rev. B* **98**, 104309 (2018).
- [29] D. C. Rose, H. Touchette, I. Lesanovsky, and J. P. Garrahan, *Phys. Rev. E* **98**, 022129 (2018).
- [30] S. Belan and V. Parfenyev, *New Journal of Physics* **22**, 073065 (2020).
- [31] A. Riera-Campenya, J. Ollé, and A. Masó-Puigdellosas, [arXiv:2011.04403](https://arxiv.org/abs/2011.04403) (2020).
- [32] G. Peretto, F. Carollo, M. Magoni, and I. Lesanovsky, *Phys. Rev. B* **104**, L180302 (2021).
- [33] G. Peretto, F. Carollo, and I. Lesanovsky, *SciPost Phys.* **13**, 079 (2022).
- [34] X. Turkishi, M. Dalmonte, R. Fazio, and M. Schirò, *Phys. Rev. B* **105**, L241114 (2022).
- [35] D. Das, S. Dattagupta, and S. Gupta, *Journal of Statistical Mechanics: Theory and Experiment* **2022**, 053101 (2022).
- [36] M. Magoni, F. Carollo, G. Peretto, and I. Lesanovsky, *Phys. Rev. A* **106**, 052210 (2022).
- [37] R. Yin and E. Barkai, *Phys. Rev. Lett.* **130**, 050802 (2023).
- [38] R. Yin and E. Barkai, [arXiv:2301.06100](https://arxiv.org/abs/2301.06100) (2023).
- [39] R. Modak and S. Aravinda, [arXiv:2303.03790](https://arxiv.org/abs/2303.03790) (2023).
- [40] A. Acharya and S. Gupta, [arXiv:2308.14040](https://arxiv.org/abs/2308.14040) (2023).
- [41] M. Kulkarni and S. N. Majumdar, [arXiv:2305.15123](https://arxiv.org/abs/2305.15123) (2023).
- [42] M. Kulkarni and S. N. Majumdar, [arXiv:2307.07485](https://arxiv.org/abs/2307.07485) (2023).
- [43] P. Chatterjee, S. Aravinda, and R. Modak, [arXiv:2311.09150](https://arxiv.org/abs/2311.09150) (2023).
- [44] D. A. Puente, F. Motzoi, T. Calarco, G. Morigi, and M. Rizzi, [arXiv:2305.08641](https://arxiv.org/abs/2305.08641) (2023).
- [45] F. Liu, [arXiv:2308.02214](https://arxiv.org/abs/2308.02214) (2023).
- [46] F. A. Grünbaum, L. Velázquez, A. H. Werner, and R. F. Werner, *Communications in Mathematical Physics* **320**, 543 (2013).
- [47] H. Krovi and T. A. Brun, *Phys. Rev. A* **74**, 042334 (2006).
- [48] S. Dhar, S. Dasgupta, and A. Dhar, *Journal of Physics A: Mathematical and Theoretical* **48**, 115304 (2015).

- [49] S. Dhar, S. Dasgupta, A. Dhar, and D. Sen, *Phys. Rev. A* **91**, 062115 (2015).
- [50] H. Friedman, D. A. Kessler, and E. Barkai, *Phys. Rev. E* **95**, 032141 (2017).
- [51] F. Thiel, E. Barkai, and D. A. Kessler, *Phys. Rev. Lett.* **120**, 040502 (2018).
- [52] S. Lahiri and A. Dhar, *Phys. Rev. A* **99**, 012101 (2019).
- [53] R. Yin, K. Ziegler, F. Thiel, and E. Barkai, *Phys. Rev. Research* **1**, 033086 (2019).
- [54] F. Thiel, I. Mualem, D. Meidan, E. Barkai, and D. A. Kessler, *Phys. Rev. Research* **2**, 043107 (2020).
- [55] F. Thiel, I. Mualem, D. A. Kessler, and E. Barkai, *Phys. Rev. Research* **2**, 023392 (2020).
- [56] P. Kuklinski, *Phys. Rev. A* **101**, 032309 (2020).
- [57] F. Thiel, I. Mualem, D. Kessler, and E. Barkai, *Entropy* **23**, 595 (2021).
- [58] D. A. Kessler, E. Barkai, and K. Ziegler, *Phys. Rev. A* **103**, 022222 (2021).
- [59] K. Ziegler, E. Barkai, and D. A. Kessler, *Journal of Physics A: Mathematical and Theoretical* **54**, 395302 (2021).
- [60] V. Dubey, C. Bernardin, and A. Dhar, *Phys. Rev. A* **103**, 032221 (2021).
- [61] A. Didi and E. Barkai, *Phys. Rev. E* **105**, 054108 (2022).
- [62] Q. Liu, K. Ziegler, D. A. Kessler, and E. Barkai, *Phys. Rev. Res.* **4**, 023129 (2022).
- [63] D. Das and S. Gupta, *Journal of Statistical Mechanics: Theory and Experiment* **2022**, 033212 (2022).
- [64] Y.-J. Wang, R.-Y. Yin, L.-Y. Dou, A.-N. Zhang, and X.-B. Song, *Phys. Rev. Res.* **5**, 013202 (2023).
- [65] Z. Ni and Y. Zheng, *Entropy* **25**, 1231 (2023).
- [66] B. Walter, G. Peretto, and A. Gambassi, *arXiv:2311.05585* (2023).
- [67] S. Tornow and K. Ziegler, *Phys. Rev. Res.* **5**, 033089 (2023).
- [68] L. Laneve, F. Tacchino, and I. Tavernelli, *Quantum* **7**, 1056 (2023).
- [69] B. Misra and E. C. G. Sudarshan, *Journal of Mathematical Physics* **18**, 756 (1977).
- [70] M. N. Jayakody, I. L. Paiva, A. Nanayakkara, and E. Cohen, *Phys. Rev. A* **105**, 032413 (2022).
- [71] T. R. Gingrich and J. M. Horowitz, *Phys. Rev. Lett.* **119**, 170601 (2017).
- [72] J. P. Garrahan, *Phys. Rev. E* **95**, 032134 (2017).
- [73] G. Falasco and M. Esposito, *Phys. Rev. Lett.* **125**, 120604 (2020).
- [74] A. Pal, S. Reuveni, and S. Rahav, *Phys. Rev. Res.* **3**, L032034 (2021).
- [75] Y. Hasegawa, *Phys. Rev. E* **105**, 044127 (2022).
- [76] R. Bebon and A. Godec, *Phys. Rev. Lett.* **131**, 237101 (2023).
- [77] O. L. Bonomo and A. Pal, *Phys. Rev. E* **103**, 052129 (2021).
- [78] C. Cohen-Tannoudji, B. Diu, and F. Laloë, *Quantum Mechanics, Volume 1: Basic Concepts, Tools, and Applications* (Wiley, 2019).
- [79] E. Bäumer, V. Tripathi, D. S. Wang, P. Rall, E. H. Chen, S. Majumder, A. Seif, and Z. K. Mineev, *arXiv:2308.13065* (2023).
- [80] A. Montanaro, *Theory of Computing* **14**, 1 (2018).

ACKNOWLEDGMENTS

We acknowledge the use of IBM Quantum services. The views expressed in this work are those of the authors and do not reflect the official policy or position of IBM or the IBM Quantum team. Q.W. and R.Y. acknowledge the use of the IBM Quantum Experience and the IBMQ-research program. Q.W. would like to thank the Max Planck Institute for the Physics of Complex Systems for its hospitality. The support of Israel Science Foundation's grant 1614/21 is acknowledged.

AUTHOR CONTRIBUTIONS

E.B. and S.T. conceived and designed the project. R.Y., Q.W. and E.B. constructed the theory. Q.W. and S.T. performed the experiments and data analysis. R.Y. and Q.W. generated numerical simulations. All authors discussed the results. R.Y., Q.W., S.T. and E.B. contributed to the manuscript.

COMPETING INTERESTS

The authors declare no competing interests.